The use of inverse methodologies in geotechnical problems

António Tavares de Castro, N. S. Lenao, Luís Ribeiro E Sousa, Defeng Desheng, D. Nguyen-Minh

The Use of Inverse Methodologies in Geotechnical Problems

by A.T. Castro[1], N.S. Leitão[1], L. Ribeiro e Sousa[2], D. Desheng[3] & Nguyen-Minh D.[4]

Introduction

Back analysis problems, also known as inverse problems or characterization problems, can be formulated as parameter estimation problems, by which means two basic types of problems can be solved:

i) Determination of external loads from the structural properties and from observed response, sometimes called inverse problems of the first kind;

ii) Determination of structural properties parameters as a function of the external loads and observed responses, sometimes called inverse problems of the second kind.

The structural properties are defined by the geometry of the structure and by the properties and zoning of the different constituent materials. The observed effects (displacements, unit strains, stresses, etc.) represent the structural response. The former type of problems corresponds to the determination of the actions on basis of structural properties and of observed effects, whereas the latter refer to the determination of the characteristics parameters of the structural properties on basis of actions and corresponding observed effects.

Back analysis problems can be solved in two ways, which Cividini calls direct approach and inverse approach (Cividini et al., 1981).

The direct approach uses the same numerical solutions as the direct analysis, determining the values of the parameters in accordance to some identification criteria, corresponding, for instance, to the least square, Markov or maximum likelihood methods (Eykhoff, 1974). The inverse approach requires a reformulation of the problem equations in such a form that the observed effects correspond to known quantities whereas the parameters to be identified appear as unknown.

Direct approach methodologies allow the identification of model parameters related with actions or with structural properties (in particular, with material properties), which includes the combined use of a numerical model and of an adequate minimization method. This approach is less sensitive to the quality of the observed values and to the degree of approximation of the numerical model. An important feature of these methodologies is the separate use of the numerical model and of the minimization method, which allow the use of complex models developed in commercial programs (without access to its code).

Inverse approach methodologies allow, in principle, faster convergence taxes than direct approach methodologies. Nevertheless, these methodologies are more sensitive to the quality and to the quantity of the observed effects and require numerical models that can reproduce approximately the observed response. Usually, the resolution of specific problems requires the development of specific codes since it is difficult or even impossible to adapt commercial programs to this purpose.

In the next paragraphs three different back analysis approaches will be presented.

1. LNEC—Laboratório Nacional de Engenharia Civil, Lisbon, Portugal
2. LNEC & University of Porto, Portugal
3. Research Center of Hydraulic Structures, Hohai University, Nanjing, China
4. Laboratoire de Mécanique des Solides, Ecole Polytechnique, Palaiseau, France

General Direct Back Analysis Methodology, Based on the Minimization of an Objective Function

Mathematical Formulation

This approach can be developed in two stages (Castro, 1998):

i) the formulation of an objective function to minimize according to same identification criteria;

ii) the minimization of this objective function.

The maximum likelihood criteria of identification it is the more general. Assuming as correct a deterministic model that relates the unknown parameters ($\mathbf{p}$) to the responses ($\mathbf{y}_M(\mathbf{p})$), the differences between these responses and the correspondent measurements ($\mathbf{y}_O$) can be considered as an error and defined in a probabilistic manner. Therefore the probability of reproducing the measurements given a set of parameters ($P(\mathbf{y}_O|\mathbf{p})$) is equal to the probability of reproducing the error measurements ($P(\mathbf{y}_O-\mathbf{y}_M(\mathbf{p}))$),

$$P(\mathbf{y}_O|\mathbf{p}) = P(\mathbf{y}_O - \mathbf{y}_M(\mathbf{p})) = \frac{|\mathbf{C}_u|^{-1/2}}{(2\pi)^{m/2}} \exp\left(-\frac{1}{2}(\mathbf{y}_O-\mathbf{y}_M(\mathbf{p}))^T \mathbf{C}_u^{-1}(\mathbf{y}_O-\mathbf{y}_M(\mathbf{p}))\right) \quad (1)$$

where m represents the number of measurements and $\mathbf{C}_u$ is the measurements covariance matrix,

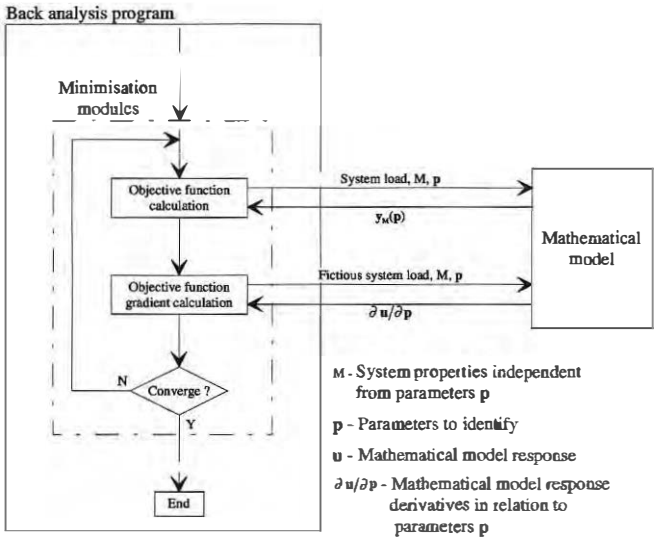

Figure 1. Back analysis computational system.

which represents the structure of the error measurements. As $P(\mathbf{y}_O|\mathbf{p})$ is a monotonic function on $\mathbf{p}$, its maximum is obtained minimising its logarithm. If the covariance matrix does not depend on $\mathbf{p}$, an objective function of the form

$$\psi(\mathbf{p})=(\mathbf{y_o}-\mathbf{y_M}(\mathbf{p}))^T\mathbf{C_u^{-1}}(\mathbf{y_o}-\mathbf{y_M}(\mathbf{p})) \quad (2)$$

is obtained.

If the measurements are independent and their errors have a Gaussian distribution with variance σ^2, the covariance matrix takes the form

$$\mathbf{C}_u=\sigma^2\mathbf{I} \quad (3)$$

where $\mathbf{I}$ is the identity matrix. In this case, the minimum of equation (2) is equal to the minimum of the objective function obtained by the least squares method

$$\psi(\mathbf{p})=(\mathbf{y_o}-\mathbf{y_M}(\mathbf{p}))^T(\mathbf{y_o}-\mathbf{y_M}(\mathbf{p})) \quad (4)$$

Then, any minimisation method that allows taking into account the numerical nature of the mathematical models can be used. If gradient methods are used, the gradient of the objective function can be determined by difference finite methods or numerically calculated through the response of the model to fictitious loads.

In terms of computational implementation, it is useful to separate the back analysis modules from the modules correspondents to the numerical model, which requires only writing interface routines between the two groups of modules allowing the use of mathematical models built with commercial programs (Figure 1).

Identification of Funcho Dam Foundation Deformability

Funcho Dam (Figure 2) is part of the Algarve Hydraulic Project for irrigation and water supply purposes. It consists of a thin double curvature arch dam with a maximum height of 43m, supported by a foundation pulvino and two artificial abutments. The insertion of the dam in the valley is asymmetric but the foundation plinth and the abutments

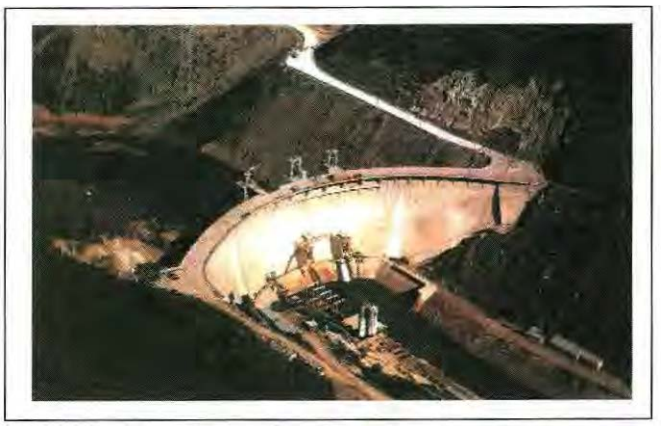

Figure 2. Funcho dam

allow the arch to be symmetric. The principal characteristics of the arch are:

Height above the plinth . . . . . .35.0 m
Crest length . . . . . .165.0 m
Thickness (central cantilever base) . . . . . .6.4 m
Thickness (central cantilever crest) . . . . .2.25 m

The foundation of the dam presents great lithologic heterogeneities. It consists of meta-sandstone and greywacke with small intercalations of schist in the left bank and of schist with intercalations of graphytic phyllite in the right bank. In terms of deformability the average values for the two banks are very different and there are significative variations along the insertion of the dam in the foundation. In situ tests with large flat jacks (LFJ) and borehole dilatometers (BHD) indicates modules of elasticity of 0.5 to 15 GPa for the schist and of 32 to 46 GPa for the greywacke.

In accordance with the monitoring plan of the dam, eight groups of rockmeters were installed along the foundation during the construction of the structure. These devices provide measurements of relative displacements between the base of the dam and points situated at depths that correspond to 75% of the dam height. Some of these rockmeters have one additional reference point situated at depths that correspond to 30% of the dam height. In all sections the rockmeters are placed in the drainage gallery (upstream), but, in some cases, there is one additional rockmeter installed downstream, at the end of radial galleries (Figure 3).

To identify the foundation deformability parameters of Funcho dam, the displacements observed in upstream rockmeters of groups GEF2 to GEF8 during the two last semesters of construction were considered (Castro, 1998). The more significative settlements in the right bank, show the asymmetry of the foundation deformability between the two banks.

The dam's behaviour was simulated by a thin shell model, elastically supported on the foundation, analysed by the finite element method. The concrete of the dam was supposed homogeneous and isotropic, with an elastic behaviour characterised by a module of elasticity of 25 GPa and a Poisson ratio of 0.2. The foundation was divided in zones constituted by greywacke or schist. In each of

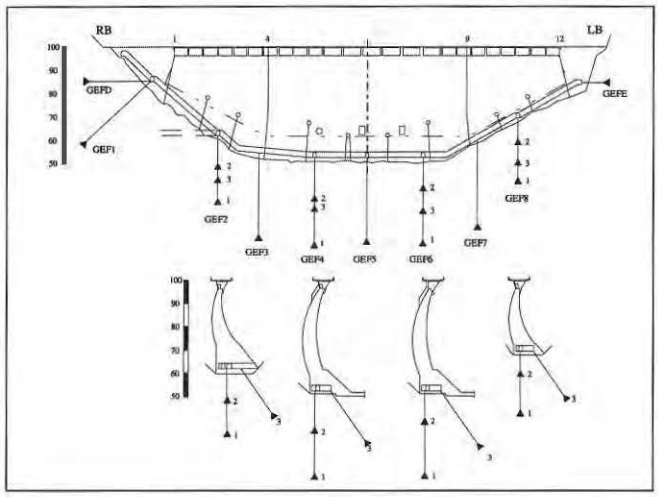

Figure 3. Funcho dam. Rockmeters localization.

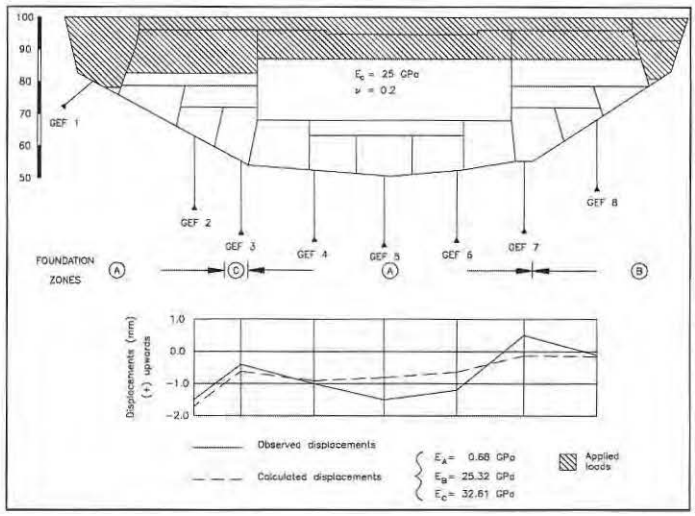

Figure 4. Funcho dam. Back analysis results.

them, the materials were considered homogeneous, isotropic and with elastic behaviour. The deformability of the foundation was considered by means of Vogt coefficients (USBR, 1948).

Figure 4 shows the zoning of the foundation and the applied loads (dead weight of upper blocks). The results plotted in this figure indicate that the right bank and the centre of the valley have a low modulus of elasticity (less than 1 GPa), the left bank a modulus of elasticity of 25 GPa and that there are a small but significant rigid zone at the bottom of the right bank. Taking into account the precision of the measured values, the approximations of the adopted model and the fact that no displacements were observed at the top of the banks, the calculated displacements fit satisfactory the correspondent observed values.

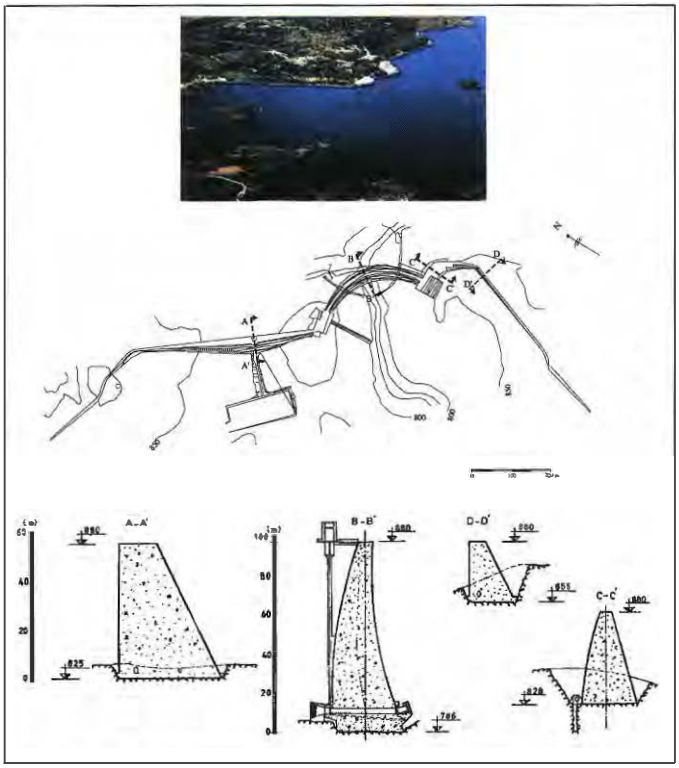

Figure 5. Alto Rabagão dam. Plan and cross sections (PNCOLD, 1992).

Identification of Alto Rabagão Dam Foundation Permeability

Alto Rabagão is a concrete dam located in the Cávado River, in the north of Portugal (Figure 5). The dam integrates a hydroelectric development, which includes an underground powerhouse, at a depth of 130 m. The dam has three parts, namely one asymmetric arch in the central valley and two gravity structures towards the embankments, forming a reservoir with a volume of 569×10^6 m^3 and an area of 22×10^6 m^2 (Figure 5). The arch dam has a maximum height of 94 m and the more important gravity dam, located in the right bank, has a maximum height of 59 m. The dam has a total volume of concrete of 1 129 000 m^3 and was built between 1958 and 1965 (PNCOLD, 1992).

The dam is supported by a weathered granite rock with some schist veins, which has some very altered zones. The main discontinuities are three sets of joints, two subverticals and one subhorizontal, and some faults of little importance. The estimated deformabilities of the foundation were 20GPa for the right bank and 1GPa for the left one. Taking into account these characteristics, extensive consolidation work through the injection of cement grouts was executed.

The study of the hydraulic properties of the foundation has been more limited, but some in situ tests showed permeabilities around 3.6×10^{-6} ms^{-1}, with minimum values of 4.5×10^{-8} ms^{-1}. An impermeabilization curtain was built through the injection of cement grouts. The curtain boreholes were drilled until a depth corresponding to permeability less than a 1 Lugeon, with a minimum value of 35m in rock. The drainage curtain was designed to avoid water resurgences downstream of the dam and high gradients in the upstream zone of the foundation.

Two curtains were executed: the primary curtain in the downstream gallery of the dam and the secondary curtain in the downstream toe. To observe the uplift pressures in the foundation, piezometers were installed between the drainage boreholes of the primary curtain. In the blocks with radial gal-

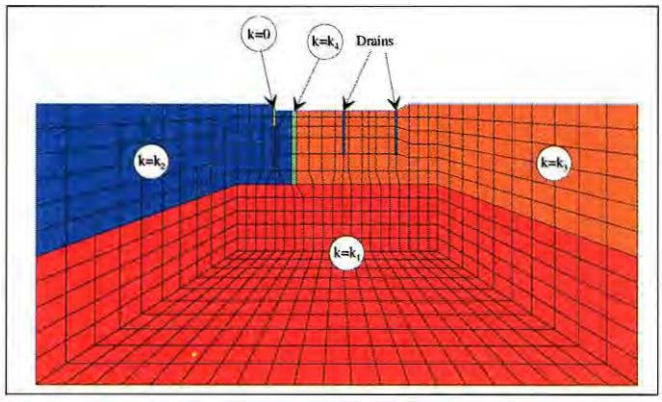

Figure 6. Hydraulic model of the foundation

leries piezometers groups were installed through the upstream-downstream direction.

During the first filling of the reservoir, which took place between December 1965 and March 1966, the monitoring results pointed to a satisfactory behaviour of the foundation.

During the lifetime of concrete dams the hydraulic characteristics can change significantly due to mechanical and chemical actions associated with the water flow in the rock mass. Therefore, it is important to evaluate periodically the hydraulic properties of the rock mass.

Although this evaluation is usually made by in-situ Lugeon type tests, like the ones performed during the design stage, it is also possible to identify the permeabilities by back analysis methods.

In this study (Castro, 1998), a mathematical plane model solved by the finite difference method (ITASCA, 1995) has been used to represent the hydraulic behaviour of the foundation of the block 11–12 of the right bank gravity dam (section C–C'). The model considers an area of 225×100 m² under the base of the block and assumes material with homogeneous and isotropic hydraulic properties and a laminar flow in accordance with the Darcy law. The waterproofing grout curtain is represented by a group of elements of unknown permeability and the drain and piezometers are represented by lines (Figure 6).

The model considers five zones, including the concrete wall in the upstream toe of the dam with permeability equal to zero and four zones whose permeabilities are to be identified (Figure 6). The fourth zone corresponds to the impermeabilization curtain ($k=k_4$).

The calculated values corresponding to the observed uplifts pressures are the mean of the pressures determined through the mathematical model for the points located along the piezometers line, discounting the height of the column of water to their top.

The calculated flow (Q_{calc}) corresponds to the sum of the values determined for the points located along the drain line. As the model is plane, to take into account the fact that the drainage curtain is constituted by individual drains with a known perimeter (p) and a known spacing (a = *10 m*), it is

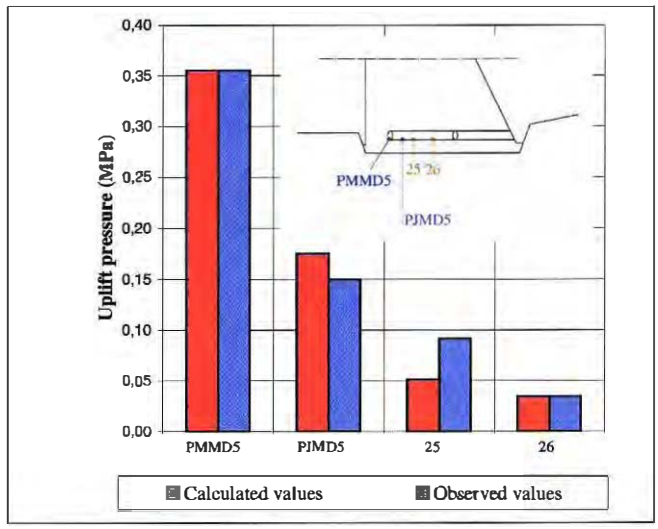

Figure 7. Observed uplifts pressures and corresponding values calculated during the back analysis iterations

necessary to determine the flow in an individual drain (Q_{dren}) by the formulae (Andrade, 1984)

$$Q_{dren} = \lambda\, Q_{calc} \quad \text{with} \quad \lambda = \frac{2\pi}{a \ln \frac{a}{p}} \tag{5}$$

As the drains have a diameter ϕ = 3" (0.0762 m), a coefficient λ = 0.1683 is obtained.

The only observed flow determine directly the global permeability of the rock mass and several observed uplifts determine the relations between the permeabilities of the different zones. As these influences are independent, the identification can be established in two stages, namely: i) determination of the relation of the permeabilities of the different zones, using only the values of the observed uplifts; ii) identification of the values of these permeabilities, using the relation between the observed and the calculated flow.

In the first stage, the least squares identification criteria and the conjugate gradient method for the minimization of the objective function were used. The gradient of the objective function was determined by the finite difference method. Comparing the observed and the calculated uplift pressures the agreement is particularly good for piezometers PMMD5 and P26, acceptable for piezometer PJMD5 and less good for piezometer P25 (Figure 7).

In the second stage the permeabilities obtained in the first one were corrected by the coefficient $\theta = Q_{dren} / Q_o$ where Q_o is the observed flow (Table 1). Figure 8 presents the head contours calculated with the identified permeabilities.

Identification of the In-situ State of Stress and the Deformability of the Rock Mass in Alto Lindoso Powerhouse Complex

The Alto Lindoso hydroelectric power scheme essentially consists of an arch dam, two parallel high pressure hydraulic circuits starting on the left bank, an underground powerhouse complex (pow-

Figure 8. Head contours calculated with the identified permeabilities.

Permeability	1st Stage (10^{-3} cm.s^{-1})	2nd Stage (Lugeons = 10^{-5} cm.s^{-1})
k_1	0.43	0.49
k_2	2.85	3.18
k_3	1.49	1.67
k_4	0.21	0.24

Table 1: Alto Rabagão dam. Identified permeabilities

erhouse cavern, spherical valve chamber and butterfly valve chamber), two draft tubes joining at the surge chamber, and a tailrace tunnel (Figure 9a).

The powerhouse, with the main floor located at a depth of 340m, is 90.0m long and 20.9m wide between vertical walls has a maximum span of approximately 33m at the ceiling, and a maximum height of about 50m.

A complete observation plan for the underground structures was implemented, mainly focused on the large underground caverns of the powerhouse complex, where three sections were monitoring with rock extensometers, Carlson type extensometers and convergence measurements (Figure 9b).

The excavation of the powerhouse complex was accomplished in a sequential way (Figure 9c).

In this analysis two components of the initial state of stress (σ_x and σ_{xy}) and the deformability of the rock mass (*E*) of the underground structures are determined. The vertical component of the initial state of stress was assumed equal to the dead weight. The monitoring results to be considered are the convergence and the displacements in the rod-extensometers $EB_{1.2}$, $EB_{4.2}$ and $EB_{8.2}$ of section S_2, measured in stages 3 and 6, and the in-situ stresses obtained by small flat jack tests (SFJ) at the end of stage 6 (Castro, 1998).

This example involves some significant particularities. On one hand, two different types of parameters (in-situ stresses and elasticity modulus) are determined on the basis of two different types of measurements (displacements and stresses); on the other hand, the computation procedure is developed in *n* different stages.

The responses ($\mathbf{y}_M(p)$) are obtained, in each stage *n*, using the displacement vector $\mathbf{u}_n$ resulting from the equilibrium of the stress field after the stress relaxation in the rock due to excavations in the previous stage. Using Finite Element equations it can be written as

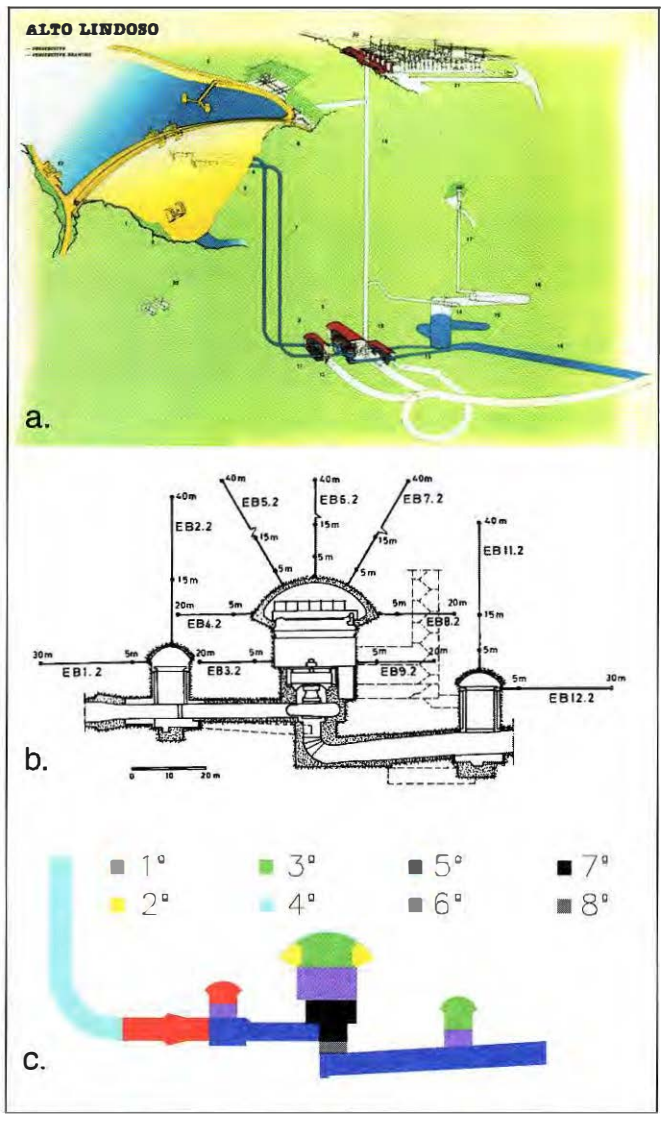

Figure 9. Alto Lindoso hydroelectric scheme.
a) Hydroelectric scheme
b) Rock extensometers in the powerhouse complex
c) Excavations stages

$$\mathbf{K}_n \mathbf{u}_n = \int \mathbf{B}_n^T \sigma_{n-1} dV \qquad (6)$$

where **K** is the stiffness matrix, **B** is a matrix of the derivatives of the shape functions and σ is the state of stress resulting from the previous stage.

Considering that the structure to be analyzed has *ne* different elasticity modulus zones and *ns* different initial state of stresses zones, the problem to be solved consists, then, in the identification of the *ne* elasticity modulus and the *ns* groups of the initial stress components.

Thus, for determining the elasticity modulus of the *i* zone, we have to derive with respect to *E* the expression (6)

$$\mathbf{K}_n \frac{\partial \mathbf{u}_n}{\partial E_i} = -\frac{\partial \mathbf{K}_n}{\partial E_i} \mathbf{u}_n + \int_V \mathbf{B}_n^T \frac{\partial \sigma_{n-1}}{\partial E_i} dV \qquad (7)$$

The derivative of the stiffness matrix is determined by assembling elementary matrixes calculat-

Parameter	Test results	Back analysis results
σ_x(MPa)	-10.7 (STT and SFJ)	-10.3
σ_{xy}(MPa)	2.9 (STT)	0.2
E(GPa)	63 (GSI)	65.0
σ_y(MPa)	-7.6 (STT and SFJ)	-9.0[1]

Table 2: Comparison between observed and calculated parameters

ed using the elasticity matrix **D** derivatives with respect to the elasticity modulus:

$$\mathbf{K}_n^e = \int_{V^e} \mathbf{B}_n^T \mathbf{D} \mathbf{B}_n dV \Rightarrow \frac{\partial \mathbf{K}_n^e}{\partial E_i} = \int_{V^e} \mathbf{B}_n^T \frac{\partial \mathbf{D}}{\partial E_i} \mathbf{B}_n dV \quad (8)$$

The stresses in the previous stage are computed from

$$\sigma_{n-1} = \sigma_{n-2} + \mathbf{D}\mathbf{B}_{n-1}\mathbf{u}_{n-1} = \sigma_{n-2} + \mathbf{S}_{n-1}\mathbf{u}_{n-1} \quad (9)$$

which after deriving with respect to E becomes

$$\frac{\partial \sigma_{n-1}}{\partial E_i} = \frac{\partial \mathbf{D}}{\partial E_i}\mathbf{B}_{n-1}\mathbf{u}_{n-1} + \mathbf{D}\mathbf{B}_{n-1}\frac{\partial \mathbf{u}_{n-1}}{\partial E_i} \quad (10)$$

Notice that equations 7 to 10 are only valid from stage 2 to n. For the first stage, the displacement derivatives are calculated by equation (11), in which case the integral on the right hand side is equal to zero as $\sigma_{n-1} = \sigma_o$ does not depend on E

$$\mathbf{K}_1 \frac{\partial \mathbf{u}_1}{\partial E_i} = -\frac{\partial \mathbf{K}_1}{\partial E_i}\mathbf{u}_1 \quad (11)$$

The derivatives with respect to the initial state of stress σ_{oi}, are performed in a similar way.

In this study a mathematical plane model solved by the finite difference method (ITASCA, 1995) is used. In Table 2 the in-situ test results and the corresponding identified values are presented. In Figure 10 the observed and the calculated responses with the identified parameters are presented.

Identification of Pressure Distribution in Campilhas Dam Gallery, Using a Method Based on the Superposition Principle

Campilhas dam is an earthfill dam, constructed for the irrigation of the agricultural soils on the banks of the Campilhas and S. Domingos rivulets. It was built during the 1950's and includes a spillway gallery, a water intake pipe and a small powerhouse.

The spillway gallery has an approximate length of 300m and a maximum overburden of about 25m. It has an internal circular section of 5m in diameter, and a water intake pipe, 1.20m in diameter, is embedded in its concrete lining.

At the end of 1994, due to the evidences of deterioration in the steel lining of the water intake circuit, the INAG—Instituto da Água—decided to carry out repair works. As the replacement of the steel lining would required to make some access openings in the concrete support of the gallery, an intensive program of studies was carried out in order to

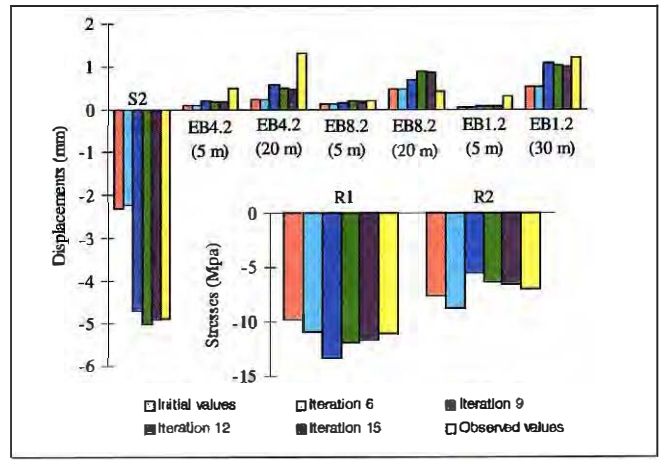

Figure 10. Comparison between observed and calculated responses.

avoid any risk of loosing structural stability during work advance.

The gallery crosses schist formations that, according to the seismic refraction profiles obtained by INAG, were characterized as varying from fair to very poor rock. Taking into consideration this geotechnical zoning of the rock mass, three measurement sections were selected at 100, 169 and 210m from the end of the gallery. For each section, three boreholes were drilled in order to obtain rock and concrete samples (Figure 11). Some of these boreholes were also observed with a closed television circuit.

The rock samples obtained were highly fractured, low values of RQD, between 10 and 15, were usually determined. For each section, three SFJ tests were carried out at the locations indicated in Figure 11. The resulting stresses are indicated in the figure. By comparing the results for these three sections it is evident that the stresses in the right sidewall were quite similar, but, in contrast, in the left sidewall and in the crown they were different.

Based on the stresses measured in sections S1, S2 and S3, the inverse problem of obtaining the external pressure distribution acting on the gallery lining was then addressed.

It was assumed that the external pressure distribution could be obtained from the superposition of the following elementary loads (Leitão et al., 1995):

- uniform distributed pressure;
- linear distributed pressure;
- parabolic distributed pressure;

applied in both, horizontal and vertical directions. Therefore, the stress at any point within the support could be determined from the expression

$$\sigma(P_i) = \sum_{j=1}^{m} \xi_j \sigma_j(P_i) \quad (12)$$

where ξ_j is the weight coefficient of the elementary load j, $\sigma_j(P_i)$ is the stress at point P_i due to the load j, and m represents the total number of elementary loads considered.

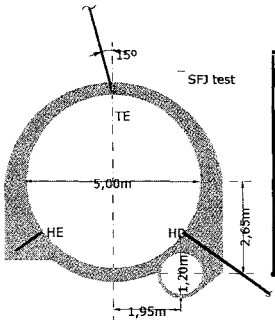

Test	Stress (MPa)		
	Section S1	Section S2	Section S3
HE	-1.0	-2.7	-1.5
HD	-1.1	-1.0	-0.9
TE	-0.4	-5.3	-4.2

Figure 11. Locations and results of the boreholes and SFJ tests.

Since this approach is based on the superposition principle, both concrete and rock must be assumed to behave as linear elastic materials.

The analysis was performed in the following way:

1. Elementary loads definition: six different elementary loads were considered, three acting in the horizontal direction and the other three in the vertical one (Figure 12).

2. Solution of the elementary loads: for each elementary load the circumferential stress was computed at the points where SFJ tests were performed. These calculations were carried out using numerical analysis performed with the two-dimensional finite difference code *FLAC* (ITASCA, 1995).

3. System of equations: with the stresses computed in the previous step, a matrix $\mathbf{A}=[a_{ij}]$ (i=1,2,3; j=1,2,...,6) was defined where the element aij represents the circumferential stress at the point P_i due to the elementary load j. Then, for each section being analysed the following system was formed

$$\sum_{j=1}^{6} a_{ij}\xi_j = c_i \tag{13}$$

4. Solution of the system of equations: as the above system of equations is underdetermined, i.e., it has more unknowns than equations, there is more than one possible solution. To solve this system, two different techniques were used: normal

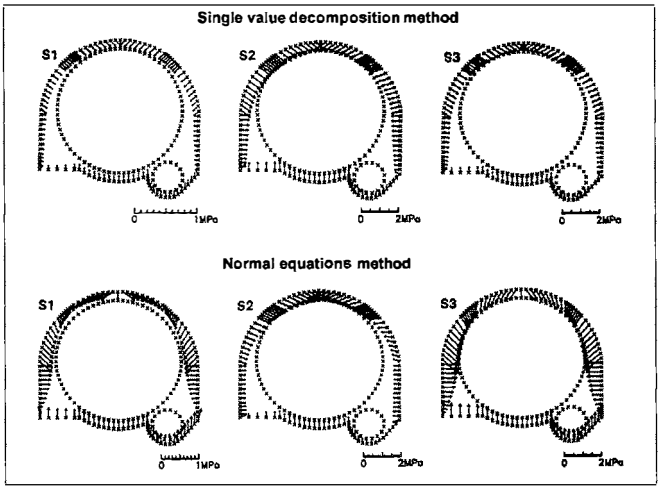

Figure 13. External pressure distribution

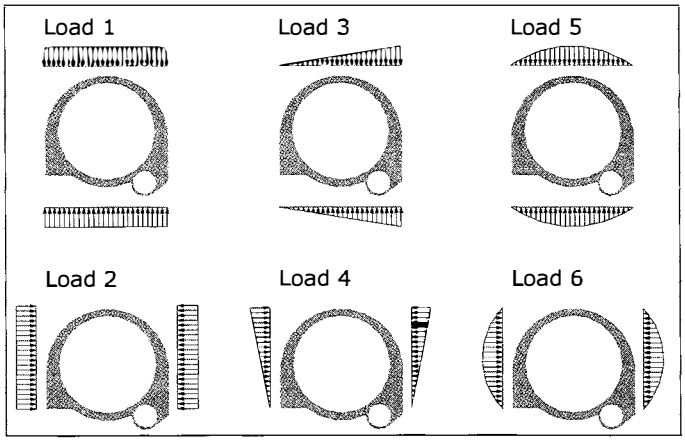

Figure 12. Elementary loads

equations (NE) and singular value decomposition (SVD).

In Figure 13, the external pressure distribution, for each section, obtained from the two techniques is shown.

Back Analysis On Mechanical Behavior Of Joints, Using A Method Based On Virtual Work Principle

Mathematical formulation (Deng et al., 2001)

A joint Γ_j separates the domain Ω into the two subdomains Ω_1 and Ω_2, $\Omega=\Omega_1\cup\Omega_2\cup\Gamma_j$ (Figure14). During a certain time interval $[0, t_0]$, the initial state and the history of displacement limit condition (on $\Gamma_u \times [0, t_0]$) and the surface force $\mathbf{T}$ (on $\Gamma_T \times [0, t_0]$) are known.

At time t = 0, the initial state in the domain is:

$$\begin{cases} \mathbf{u}(x,0) = 0 & x \in \Omega \\ \boldsymbol{\sigma}(x,0) = \boldsymbol{\sigma}_0(x) & x \in \Omega \\ \mathbf{T}(x,0) = \mathbf{T}_0(x) & x \in \Gamma_T \end{cases} \tag{14}$$

where $\mathbf{u}$ and σ are displacement and stress respectively.

Let us consider a virtual displacement field $\hat{u}(x)$ and the corresponding deformation field $\hat{\varepsilon}(x)$, which is continuous and continuously differentiable in Ω_1 and Ω_2. Suppose the stress field is continuous on Γ_j,

$$\begin{cases} \mathbf{T}_{\Omega_1}(x,t) = \boldsymbol{\sigma}(x,t).\mathbf{n}_1(x) & x \in \Gamma_j \\ \mathbf{T}_{\Omega_2}(x,t) = \boldsymbol{\sigma}(x,t).\mathbf{n}_2(x) & x \in \Gamma_j \end{cases} \tag{15}$$

The virtual work principle gives the following formula (Salençon, 1994):

$$\int_{\Omega'} \boldsymbol{\sigma}(x,t) : \hat{\boldsymbol{\varepsilon}}(x) d\Omega - \int_{\Gamma_T} \mathbf{T}(x,t).\hat{\mathbf{u}}(x) ds + \\ + \int_{\Gamma_j} \mathbf{u}_j \sigma(x,t).\mathbf{n}(x) ds = 0 \qquad t \in [0, t_0] \tag{16}$$

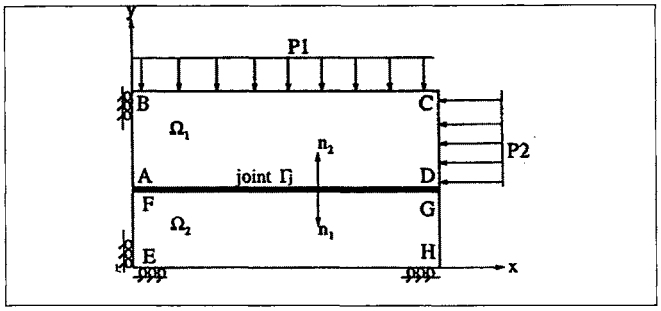

Figure 14. Numerical joint model

where $\mathbf{u}_j$ is the relative displacement between the joint interface.

Considering some displacements measurements on the border $\Gamma_T \supset \Gamma'_T$ and the limit conditions of the problem, we obtain:

$$\int_{\Omega'} (\boldsymbol{\sigma}(x) - \boldsymbol{\sigma}_0(x)) : \boldsymbol{\varepsilon}(x) d\Omega - \int_{\Gamma_T} (\mathbf{T}(x) - \mathbf{T}_0(x)) \mathbf{u}(x) ds + \\ + \int_{\Gamma_j} [[\mathbf{u}]] (\boldsymbol{\sigma}(x) - \boldsymbol{\sigma}_0(x)) \mathbf{n}(x) ds = 0 \quad (17)$$

In elastic phase, the constitutive equation of the Goodman elastic joint is defined as (Goodman, 1976):

$$\boldsymbol{\sigma}.\mathbf{n}\,|_{\Gamma_j} = \mathbf{K}[[\mathbf{u}]] \quad (18)$$

where **K** is the matrix of the elastic modulus of the joint, characterized by the normal and the tangential stiffness (k_n and k_s) and $[[\mathbf{u}]]=(u_n, u_s)^T$, with u_n and u_s the normal and tangential displacement components.

At failure, the standard Mohr-Coulomb plastic criterion,

$$\sigma_f = c + \sigma_n \operatorname{tg}\phi \quad (19)$$

is used, where σ_f is the failure limit of the tangential stress σ_s, σ_n is the normal stress component, c and ϕ are respectively, the cohesion and the friction angle of the interface.

After each solution of the problem, the elastic and the plastic zones (Γ_j^e and Γ_j^p) of the joint are determined. The basic equation of the back analysis is obtained from anterior equations as following:

$$\int_{\Omega'} (\boldsymbol{\sigma} - \boldsymbol{\sigma}_0) : \boldsymbol{\varepsilon}\ dx - \int_{\Gamma_T} (\mathbf{T} - \mathbf{T}_0).\mathbf{u}\ dx + \\ + \int_{\Gamma_j^e} k_n u_n^2 dx + \int_{\Gamma_j^p} (\sigma_n - \sigma_n^0) u_n dx + \int_{\Gamma_j^e} k_s u_s^2 dx + \quad (20) \\ + \int_{\Gamma_j^p} (\sigma_n tg\ + c - \sigma_s^0) u_s dx = 0$$

Using this equation, one parameter (k_n, k_s, c and ϕ) can be back analysed if the other parameters are supposed to be known. The algorithm of back analysis consists of:

i) Initialise the parameter to be identified

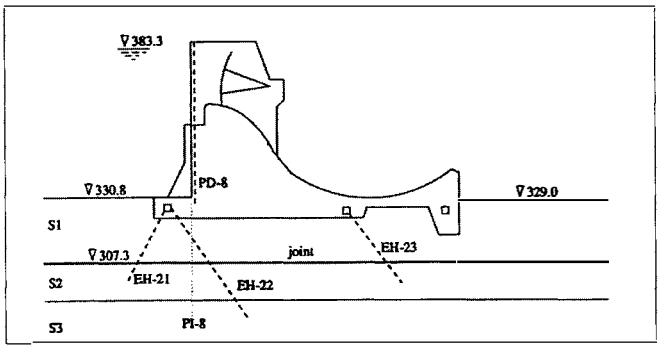

Figure 15. Água Vermelha dam

ii) Solve the problem with given parameter

iii) Update the parameter

iv) Control the iteration convergence.

Identification of the Joint Parameters in the Água Vermelha Dam Foundation

The Água Vermelha Hydroelectric Project was built on the Rio Grande river with 1380 MW installed capacity. The project comprises a 90m maximum height and 600m long concrete gravity dam and two lateral embankments (BCOLD, 1988). The designed water level is 383.3m. At the foundation of the concrete dam, there exist some discontinuities. A major horizontal joint (with clayey fillings) located at the elevation of 307.3m was very important for the deformation and safety of the dam. The dam foundation was instrumented with multiple position extensometers (EH), direct and inverted pendulums (PD and PI), piezometers, and joint displacement devices, during the construction period and reservoir filling (Figure 15). Special care was dedicated to the monitoring of Central Wall and Spillway foundation.

In this study, block section VS–8 of the spillway section is analysed with the hypothesis of plane strain problem. The concrete and rock masses are taken as elastic linear, and the joint is elastoplastic with Mohr-Coulomb plastic criterion. The displacement measurements during the reservoir filling period are listed in Table 3. Mechanical parameters are listed in Table 4, according to in-situ and laboratory tests.

Back Analysis of Elastic Parameters of Joint

Using the above measurements, the elastic stiffness k_n, and k_s, of the joint are back analysed. The initial state is selected that the gravity weight and 341.48m upstream water level were applied. Relative measurements from water level 341.48m to 360m, and from water level 360m to 376m are selected to carry out this back analysis.

After 25 iterations, the elastic joint stiffness are obtained as $k_n = 7.6\times10^8$ N/m^3 and $k_s = 1.0\times10^8$ N/m^3.

Back Analysis of Elastoplastic Parameters of Joints

For the back analysis of elastoplastic parameters of the joint, because plasticity did not occur under water level 376m, the above measurements cannot be used. Thus, a direct calculation, with mechanical parameters in Table 2 and the above back-analysed

Instrument	Water level (m)		
	341.48-360	360-370	370-376
EH-21	0.0	0.05	0.2
EH-22	0.0	0.0	-0.05
EH-23	-0.2	-0.45	-0.25
PD-8	-1.0	-0.7	-0.6
PI-8	0.2	0.1	

Table 3: Observed displacements during reservoir filling

materials	Young's modulus (MPa)	ratio	Density (T/m^3)
concrete	30000	0.20	2.5
layer S1	10000	0.20	2.9
layer S2	7000	0.20	2.9
layer S3	15000	0.20	2.9
joint	ϕ = 39° , c = 0.055 MPa		

Table 4. Mechanical parameters

elastic stiffness of the joint, is carried out with upstream water level linearly augmented to 484.7m (plasticity occurs within 47% of the joint part at the bottom of the dam). And the displacements at half the upstream surface (top part) and the surface of the dam top at water levels 464.7m (plasticity occurs within 35% of the joint part at the bottom of the dam) and 484.7m are selected as measurements.

The elastoplastic parameters ϕ and c were simultaneously back analysed for initial values: ϕ=45º, c=35000.0 Pa. Within 40 iterations, the two parameters were identified with less than 5% error: ϕ=38.9º, c=56000.0 Pa.

Final Considerations

Back analysis methods have become a useful tool in the interpretation of the observed behaviour. They are particularly helpful in cases with restricted monitoring system and little structural data, or in cases where time dependent behaviour is involved, such as the associated with the deterioration of the materials. They also represent a relevant contribution in geotechnical engineering works, such as dam foundations and underground structures, where the interpretation of the behaviour is very complex due to their discontinuity, heterogeneity and anisotropy. In this particular works, back analysis methods are not only a useful tool in the interpretation of the results of rock mass properties tests, but they are especially important in the estimation of parameters related with the characteristics of the medium during service life of the works.

References

Andrade, R. M. 1984. *Hydrogeotechnics in dams. Methods of analysis.* (in Portuguese). Engevix Rio de Janeiro, Brasil.

BCOLD 1988. *Technical data about Agua Vermelha Dam. Main Brazilian dams: design, construction and performance.* J.P. Avila, R.L. Bicudo, & F.P. Luiz (Eds.). BCOLD publications committee, Brazil. 377-407.

Castro, A. T. 1998. *Back analysis methods for the interpretation of concrete dam behaviour.* Ph.D. thesis (in Portuguese), Lisbon Technical University, Lisbon, Portugal.

Cividini, A., Jurina, L., and G. Gioda. 1981. "Some aspects of 'characterization' problems in geomechanics." *International Journal of Rock Mechanics, Mining Sciences and Geomechanics Abstracts.* 18, Pergamon Press, New York, USA.

Deng, D. and D. Nguyen Minh. 2001. *Back analysis on mechanical behaviour of joints, using a new method based on virtual work principle.* 10th Internat'l Conference of IACMAG, Arizona, USA.

Eykhoff. 1974. *System identification. Parameter and state estimation.* John Wiley & Sons, New York, USA.

ITASCA (1995). *FLAC — Fast Lagrangian Analysis of Continua.* Version 3.3. User's manual. ITASCA Consulting Group, Inc., Minneapolis, USA.

Leitão, N.S., L.R. Sousa, and L.V. Lemos. 1995. *Repairs on the water intake of the Capilhas dam.* LNEC Report (in Portuguese), Lisbon, Portugal.

PNCOLD. 1992. *Large dams in Portugal.* Portuguese National Committee on Large Dams, LNEC, Lisbon, Portugal.

Salençon, J. 1994. *Mécanique des milieux continus.* Ecole Polytechnique, Paris, France.

United States Bureau of Reclamation, USBR. 1948. *Treatise on dams.* Denver, Colorado, USA.